

# Effect of Process Parameters on the Maximum Temperature Developed and Mechanical Properties of MIG-SMD Manufactured Parts.

Adnan A. Uгла<sup>1</sup>, Ali Hatahoot Salman<sup>1\*</sup>, Ahmed Jassim Shkarah<sup>1</sup>

<sup>1</sup> Department of Mechanical Engineering, College of Engineering, University of Thi-Qar, Thi-Qar,  
64001, Iraq

\*Corresponding Author Email: alihithot@gmail.com

## Article Info

Page Number: 3775 - 3786

Publication Issue:

Vol 71 No. 4 (2022)

## Abstract

A more recent additive layered manufacturing method is shaped metal deposition (SMD). Using metal wire and a heat source like an electron beam, laser beam, or electric arc is a unique technique enabling layer-by-layer fabrication of net-shaped or near-net-shaped metal components. This paper focuses on the effect of input process parameters on the maximum temperature generated in the deposited walls and its impact on the characteristics of the final products. IR thermometer device is used to study the maximum temperature that develops throughout the deposit process and its effects on microstructure, microhardness and impact energy. Based on the Taguchi L9 orthogonal array, the selected feature matrix. And hence nine experiments were carried out. The results showed that the temperature increases with an increase in the deposit current until it arrives at a maximum value of 828 C° but decreases with increased travel speed and wire feed ratio. At the same time, the frequency parameter non-has mentioned an effect on the temperature. The average impact energy and microhardness of the deposited part at a frequency of 250 Hz reached the maximum value with the grain refining and ductile morphology at 111(Kg/mm<sup>2</sup>) and 456 HV, respectively.

**Keywords:** Shaped metal deposition, maximum temperature, microhardness, impact energy.

## Article History

Article Received: 25 March 2022

Revised: 30 April 2022

Accepted: 15 June 2022

Publication: 19 August 2022

## 1. Introduction

Similar to multi-pass welding, a manufacturing process known as shaped metal deposition (SMD) allows for the direct production of parts like flanges or lugs on already-fabricated components. The metal is deposited along a predetermined route as parts are constructed layer by layer. In order to fabricate the appropriate shape, on the substrate, a fresh layer is deposited each pass. An SMD technique produces a fine microstructure because the solidification happens quickly in a confined, restricted volume. High solidification rates are produced as a result of the filler material being cooled by conduction, mostly via the substrate (very colder) [1]. Some a researcher developed and integrated the metal wire technique and selected a heat source, such as an electric arc or beam of a laser or electron, with a new computer-aided metal deposition machine (CAMDM) and used Tungsten Inert Gas (TIG) in deposit processes[2–4]. Wire + Arc Additive Manufacturing (WAAM), which is subdivided into wire+ Metal Inert Gas (MIG) or wire + (TIG), is used in the SMD process. SMD may be manufactured using Single Wire MIG (SW-MIG) or Double Wire MIG (DW-MIG) welding. The metal deposition technique with the DW-MIG may be considered a unique and valuable way to make many metal components because of the quick deposition rates, low input of high temp produced during deposition, and reduced distortions. However, compared to laser and electron beam melting methods, the accuracy and surface finish are lower[5, 6]. To refine grains, many researchers used external excitation methods; some of them used arc oscillation, some of them used weld pool churning, and some of them used arc pulsation and used some others ultrasonic vibration.[7, 8]. IR imaging is more suitable than thermocouples for temperature recording and monitoring in weld-based AM. By using a range of experimental criteria supplied by the varied treatment of the spatial and temporal variations of temperature gathered by IR imaging, it is feasible to calibrate all the input variables for thermal simulation[9, 10]. Due to repeated heating and cooling cycling during (AM) operations and temperature distribution within the build, the structure experiences thermal stresses and strains, significantly impacting microstructure evolution. Because metal AM techniques often have substantial temperature gradients, considering elastoplastic behaviour in thermal stress analyses is critical. Thermal stress analysis begins with temperature field prediction. [11– 14].

There isa shortage of studies that experience how input process factors affect the maximum temperature developed into the deposited walls and its impact on the characteristics of the final products. In this study, an IR thermometer was used for thermal analysis inan

experimentally study, as well as mechanical properties by measurement of impact energy and microhardness using nine experiments.

## 2. Experimental Method and Materials

### 2.1 Materials and Experimental Setup

SMD machine (SMDM) used in the current study is for metal deposition procedures utilizing the DW MIG arc technique. A computer interface window with a three-axis position driven in three directions by stepper motors is used to control the created SMDM, which is combined with some other SMDM cell components to form an integrated work cell that produces the necessary parts. A 309L stainless steel wire with a 1.2 mm diameter is the material used for filling. Its grade was chosen in accordance with AWS A5.22 specifications grade FLUX-CORE. This work used two welding machines and two wire feeds, as shown in figure (1). Lincoln MIG-MAG/FLUX/BRAZING is the welding machine that provides internal hot wire to melt filler metal in the deposition zone using main heat. An external device that could be manually operated delivers a cold outer wire.



**Figure (1) Close-up view of the deposition unit.**

The experiments conducted used the consumable electrode stainless steel 309L. The grade of the wire is "E309LTI-1/T1- 4" FLUX-CORE[15]. Because it immediately covers the metal surface, this filler wire does not need the use of a shielding gas during the deposition process. C-Mn steel or

S355J2+N grade structural steel substrates with specifications BS EN 10025:2004 and ASTM A1011/1011M mild steel. A substrate with measurements of (200 \* 200 \* 5) mm was used for bead deposition.

## 2.2 Design of Experiment

Depending on the Taguchi approach employs a particular collection of orthogonal arrays that are often predefined. The Taguchi technique employs a particular set of tools to carry out a design and experience strategy. Based on the Taguchi L9 orthogonal array, the selected feature matrix, and hence nine experiments were carried out. Based on a previous study that used the same method, the sets of operational process parameters used to appear in Table (1)

**Table (1) Input Parameters with Their Levels.**

Input parameter (Symbol)	Units	Levels		
		1	2	3
Deposit Current (I)	(A)	160	190	210
Travel speed (TS)	(mm/sec)	3	4	5
Wire Ratio (WR) (W. F1*/W. F2**)	-	1.5	2	2.5
Frequency (F)	(Hz)	0	125	250

\* wire from the welding machine. \*\* Cold wire.

These values reflect the best combinations of parameters for a stable deposition process. The current work utilizes four input parameters with three levels for each.

Table (2) describes the experimental design for the Taguchi method's deposit process parameters and the outcomes, including findings for impact energy, hardness and temperature maximum.

**Table (2) Experimental Layout of Input Parameters and Responses**

Exp No.	Input parameter				Responses		
	I (A)	TS(mm /sec)	WR	F (Hz)	IE (J)	HV (Kg/mm <sup>2</sup> )	Tmax C°

1	160	3	1.5	0	79	332	765
2	160	4	2	125	95	419.8	659
3	160	5	2.5	250	111	456	695
4	190	3	2	250	96	399	790
5	190	4	2.5	0	105	394.5	721
6	190	5	1.5	125	92	405.7	677
7	210	3	2.5	125	93	406.8	828
8	210	4	1.5	250	91	405	775
9	210	5	2	0	94	364.4	807

## 2.3 Temperature and Mechanical Tests

### 2.3.1 Temperature Test

The non-contact temperature reading may be measured and displayed using an infrared thermometer (IR Thermometer) up to 2200°C (approved to 1100°C). For precise aiming and temperature monitoring, the built-in twin laser converges to a 2.54 cm target point at 127 cm. A USB PC interface, software, 100ms reaction time, Max/Min/Diff display changeable emissivity, and High/Low alarms are examples of advanced features.

### 2.3.2 Microhardness Test

The hardness of the cross-section was tested with a Vickers hardness device. The hardness test was done to show how the parameters of deposition affect the hardness. Maximum load and dwell time are 500g 10sec, respectively. After a certain number of tests, a standard test block was checked to guarantee dependability. At least three readings were taken, and the average of them, to determine the hardness of the wall in the cross-section area, as shown in Table (2).

### 2.3.3 Impact Test

The Charpy impact test (Charpy V-Notch (CVN)) is a kind of impact test used to assess the impact of toughness. By using the Charpy hammer, the overall impact work, fracture initiation work, and fracture propagation work may all be calculated. Test specimens with different cases were prepared according to the ASTM A370 standard.

### 3 Results and Discussion

#### 3.1 Max Temperature Measurement

The results were calculated from the IR thermometer and analyzed using (ANOVA). It is evident that the most important elements influencing the temperature of the deposited wall are the deposit current, with a contribution of more than 50 %, and the travel speed, with an of 39% of the overall distribution in temperature that has been seen. In contrast, the wire feed ratio and frequency factor have a minor significance.

This can be seen graphically in Figure (2), which depicts the relationship between the input parameters and the temperature. Which has a more considerable effect on the maximum temperature was the current. On the other hand, the frequency has the smallest effect with the presence of the deposit current. Also, illustrates that the increase in the current increase the temperature maximum, and that is due to the high current increasing the thermal input in the deposited wall, and that results in large grains formation, and this increase the maximum temperature values. Meanwhile, the increase in the travel speed reduces heat inputs, and that leads to the formation of refined grains, as shown in figure (2).

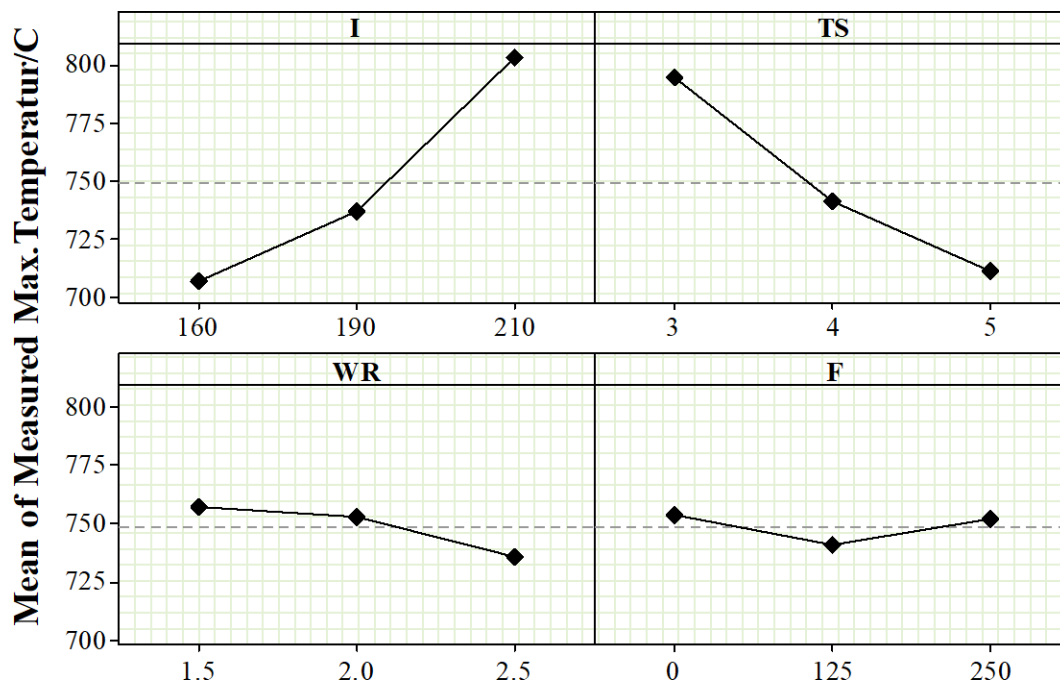
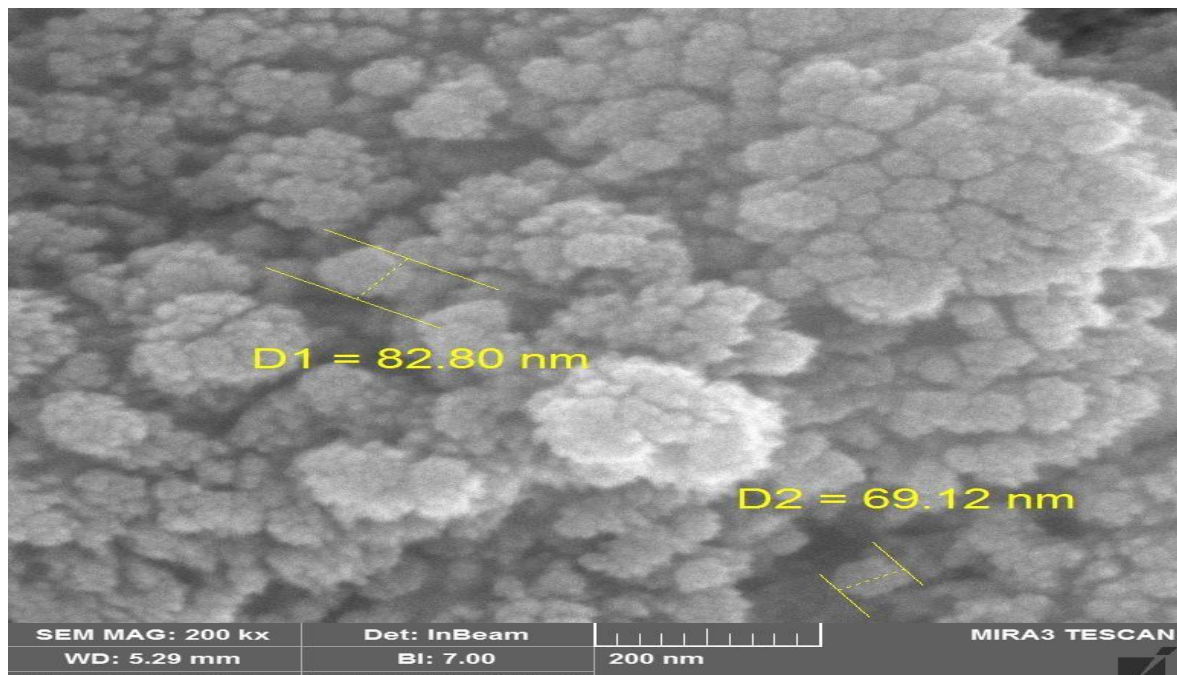


Figure. (2) Effects of main process parameters on the temperature maximum.

From the temperature test results, it was noticed that when the current increases, then the maximum temperature increases. In a direct relationship, the increase in the deposition current will increase the heat input and hence the temperature of additive layers. Also, a high current increases the elimination of the porosity in the deposition layer, which raises the maximum temperature. The model was created using a multiple regression using four regression variables and a lower squares technique (such as I, TS, WR and F).

It can be seen that the microstructure function for the heat input parameters as well as frequency level. Thus, a fine grain can be achieved with low current, high travel speed, a high amount of cold wire feed, or a high-frequency level used, as shown in Figure (3).



**Figure (3) SEM photography experiment no 3 (160 A, 5 mm/s, 2.5 and 250 Hz)**

The effect of the low travel speed, low cold wire feed, and no frequency leads to increasing the grain size in the deposited specimen. Thus, the microstructure is weak or somewhat fragile, as shown in Figure (4).

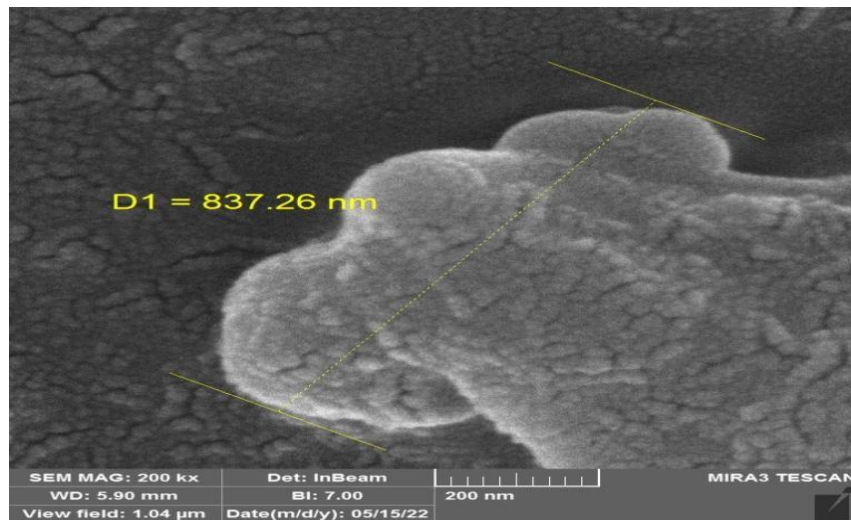


**Figure (4) SEM photography experiment no1(160 A,3 mm/s,1.5 and 0 Hz)**

### 3.2 Effect on Microhardness

The result of the analysis of variance (ANOVA) of the four main variables. The frequency has the biggest effect, with a contribution of about 50%, followed by the wire feed ratio, which has a contribution of about 22%. The travel speed, as well as the current, have less of an effect. The effects plot enables the visualization of these impacts, as shown in figure (5). Microhardness results show an increase in hardness values with increasing wire feed ratio and frequency.

This is explained by the fact that hardness rises in microstructure when refined grain composition. The microhardness relates closely to the value of frequency. It is obvious when the frequency increases, the results values of microhardness increase, which can be related to the grain refinement of the deposited part. The high frequency breaks the dendritic arms due to the distribution of heat input through the deposited evenly. Also, the high frequency increases the cooling rates, and that leads to smaller, more uniform grains, resulting in a delicate structure. While the high travel speed also affects the microhardness, when the travel speed increases, the heat input reduces, and that leads to the formation of fine grain structure and which increases the microhardness of the deposited part. The microhardness affected by the value of current can be explained through the fact that a low current value reduces the heat input, which increases the formation of the fine grain, and that increases the microhardness values.

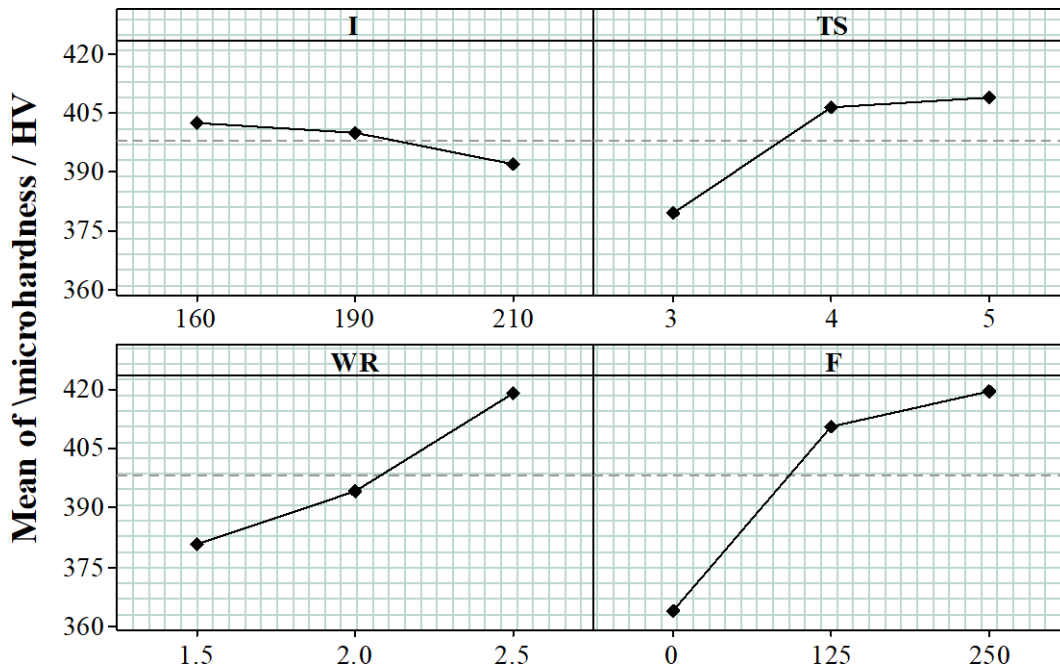


**Figure (5) The influence of key factors on microhardness.**

The result of microhardness can be summarized as the frequency and wire feed ratio had a major effect on the result. The optimum parameters for maximum hardness are high frequency, high wire ratio, high travel speed, and low depositcurrent is 456 kg/mm<sup>2</sup>.

The substrate serves as a heat sink, accelerating cooling by swiftly removing heat from the melt pool. Due to the quick heating and cooling cycles involved in the MIG plus wire deposition process, which raise thermal stress and, consequently, the dislocation density, the rapid cooling rate also results in fine microstructure and increased hardness. The model was created using a multiple regression using four regression variables and a lower squares technique.

### 3.3 Effect on Impact Energy

ANOVA analysis results of the impact test as shown in Table (4). Analyze the variation and identify the important factor impacts. It may be observed that the most significant parameters influencing impact energy are W.R and then TS, but with a small effect; this can be seen in figure (4). In contrast, other parameters are less significant. An increase in metal deposition results from an increase in W.R value, which raises impact energy. A wire feed ratio contributes

about 57%, then the travel speed with 21% of the total difference seen in the travel speed, whereas the current deposit factor has a small significance. Based on experimental data gathered from Table (2), the mathematical model was created to identify connections between impact energy and input parameters and the orthogonal array of Taguchi L9. The results of the ANOVA and the influence of the process factors can be seen on the response variables. A value of W.R significantly affects the impact of energy. Figure (6) shows that the high feed rate causes the high impact energy.

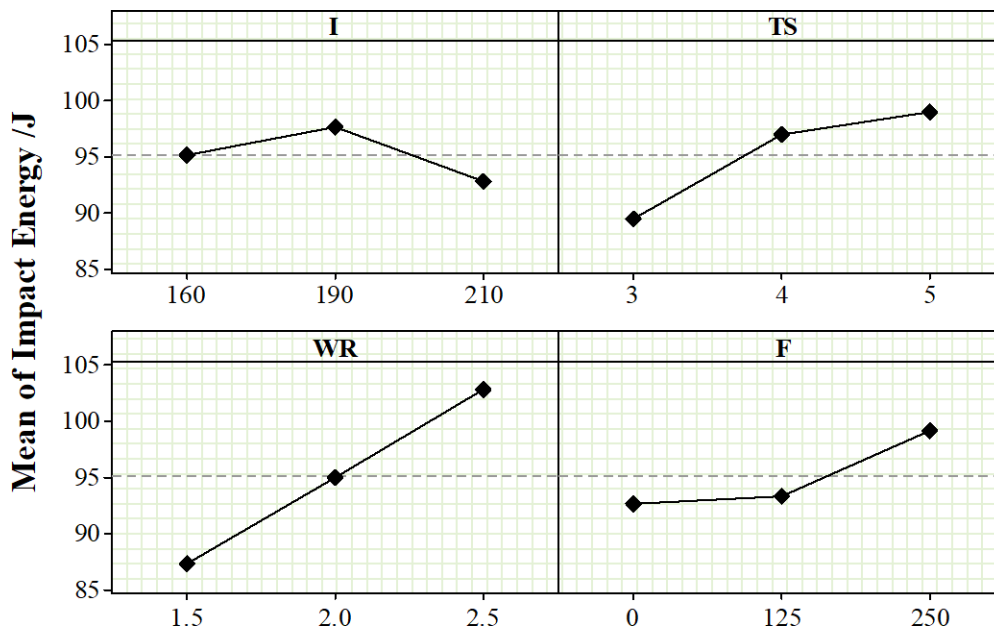


Figure. (6) Effects of main parameters on impact energy.

The reason for this is due to cold feeding, which increases the deposition rate and thus increases the deposit pass. The model was created using a multiple regression using four regression variables and a lower squares technique. (such as I, TS, WR and F).

#### 4. Conclusions

This paper used thermometer infrared, a new apparatus. This non-contact infrared thermometer monitors and displays temperatures up to 2200°C (approved to 1100°C). The sophisticated features include adjustable emissivity, a USB PC interface, software, a 100 ms response time, Max/Min/Diff displays, and High/Low alerts. The outcomes of the experiment showed that the temperature

increased through a deposition process plays a vital role in obtaining microstructure and hence affects the mechanical properties. So, it should be at a minimum as possible. The most suitable range of frequency is within (125-250 Hz), making the process less defective and more stable. The frequency is considered a significant factor affecting the microhardness. The result showed that higher frequency produces high microhardness values reaching HV=456 with frequency=250Hz. Impact energy improves by about 40% using a set of parameters as (TS 5 mm/s, WR 2.5 and F 250 Hz) in comparison to a set of (TS 3, WR 1.5 and F 0 Hz frequency used) at the same current I of 160 A. The experiments showed that all parameters had a certain effect but in different proportions on additive manufacturing processes.

#### Acknowledgement

This work was done at the Mechanical Engineering Department, Faculty of Engineering, University of Thi-Qar, Iraq.

#### References:

- [1] C. A. De Saracibar, "Encyclopedia of Thermal Stresses," *Encycl. Therm. Stress.*, no. January, 2014, doi: 10.1007/978-94-007-2739-7.
- [2] O. Yilmaz, A. R. J. Almusawi, A. A. Ugla, and O. O. Keskin, "Design, Construction, and Controlling of A Shaped Metal Deposition Machine Using Arc Metal-Wire System," no. June, 2015.
- [3] O. Yilmaz and A. A. Ugla, "Shaped metal deposition technique in additive manufacturing: A review," *Proc. Inst. Mech. Eng. Part B J. Eng. Manuf.*, vol. 230, no. 10, pp. 1781–1798, 2016, doi: 10.1177/0954405416640181.
- [4] O. Yilmaz and A. A. Ugla, "Microstructure characterization of SS308LSi components manufactured by GTAW-based additive manufacturing: shaped metal deposition using pulsed current arc," *Int. J. Adv. Manuf. Technol.*, vol. 89, no. 1–4, pp. 13–25, 2017, doi: 10.1007/s00170-016-9053-y.
- [5] A. A. Ugla, H. J. Khaidair, and A. R. J. Almusawi, "Metal Inert Gas Welding-Based-Shaped Metal Deposition in Additive Layered Manufacturing: A Review," *Int. J. Mech. Mater. Eng.*, vol. 13, no. March, pp. 244–257, 2019.
- [6] A. A. Ugla and H. J. Khaidair, "Optimization of double-wire MIG based shaped metal deposition process parameters of 3-D printed aisi 309l parts," *Int. J. Mech. Eng. Technol.*, vol.

9, no. 11, pp. 2438–2452, 2018.

- [7] A. A. Ugla, D. J. Kamil, and H. J. Khudair, “Quality Improvement of Shaped Metal Deposited Components Using Non-Traditional Techniques : a Review,” *Int. J. Mech. Prod.*, vol. 10, no. 3, pp. 2411–2430, 2020.
- [8] A. A. Ugla, D. J. Kamil, Z. A. Ibrahim, and H. J. Khudair, “Improvement Characteristics of the Shaped Metal Deposited Component Using External Excited System,” *J. Crit. Rev.*, vol. 7, no. 05, pp. 2870–2880, 2020.
- [9] X. Bai, H. Zhang, and G. Wang, “Improving prediction accuracy of thermal analysis for weld-based additive manufacturing by calibrating input parameters using IR imaging,” *Int. J. Adv. Manuf. Technol.*, vol. 69, no. 5–8, pp. 1087–1095, 2013, doi: 10.1007/s00170-013-5102-y.
- [10] X. Bai, H. Zhang, and G. Wang, “Modeling of the moving induction heating used as secondary heat source in weld-based additive manufacturing,” *Int. J. Adv. Manuf. Technol.*, vol. 77, no. 1–4, pp. 717–727, 2015, doi: 10.1007/s00170-014-6475-2.
- [11] E. Mirkoohi, J. R. Dobbs, and S. Y. Liang, “Analytical modeling of residual stress in direct metal deposition considering scan strategy,” *Int. J. Adv. Manuf. Technol.*, vol. 106, no. 9–10, pp. 4105–4121, 2020, doi: 10.1007/s00170-019-04919-0.
- [12] E. Mirkoohi, P. Bocchini, and S. Y. Liang, “Analytical temperature predictive modeling and non-linear optimization in machining,” *Int. J. Adv. Manuf. Technol.*, vol. 102, no. 5–8, pp. 1557–1566, 2019, doi: 10.1007/s00170-019-03296-y.
- [13] E. Mirkoohi, J. Ning, P. Bocchini, O. Fergani, K. N. Chiang, and S. Y. Liang, “Thermal modeling of temperature distribution in metal additive manufacturing considering effects of build layers, latent heat, and temperature-sensitivity of material properties,” *J. Manuf. Mater. Process.*, vol. 2, no. 3, 2018, doi: 10.3390/jmmp2030063.
- [14] E. Mirkoohi, D. Li, H. Garmestani, and S. Y. Liang, “Residual stress modeling considering microstructure evolution in metal additive manufacturing,” *J. Manuf. Process.*, vol. 68, no. PA, pp. 383–397, 2021, doi: 10.1016/j.jmapro.2021.04.041.
- [15] J. Luk-Cyr, R. El-Bawab, J. Lanteigne, H. Champlaud, and A. Vadean, “Mechanical properties of 75% Ar/25% CO<sub>2</sub> flux-cored arc welded E309L austenitic stainless steel,” *Mater. Sci. Eng. A*, vol. 678, pp. 197–203, 2016.